The mycobacterial acyltransferase PapA5 is required for biosynthesis of cell wall-associated phenolic glycolipids

Sivagami Sundaram Chavadi,[1]† Kenolisa C. Onwueme,[2]†‡ Uthamaphani R. Edupuganti,[1] Jeff Jerome,[1] Delphi Chatterjee,[3] Clifford E. Soll[4] and Luis E. N. Quadri[1]

Correspondence
Luis E. N. Quadri
LQuadri@brooklyn.cuny.edu

[1]Department of Biology, Brooklyn College – City University of New York, Brooklyn, NY 11210, USA

[2]Department of Microbiology and Immunology, Weill Medical College of Cornell University, NY 10021, USA

[3]Microbiology, Immunology and Pathology Department, College of Veterinary Medicine and Biomedical Sciences, Colorado State University, Fort Collins, CO 80523, USA

[4]Chemistry Department, Hunter College – City University of New York, NY 10065, USA

Phenolic glycolipids (PGLs) are non-covalently bound components of the outer membrane of many clinically relevant mycobacterial pathogens, and play important roles in pathogen biology. We report a mutational analysis that conclusively demonstrates that the conserved acyltransferase-encoding gene *papA5* is essential for PGL production. In addition, we provide an *in vitro* acyltransferase activity analysis that establishes proof of principle for the competency of PapA5 to utilize diol-containing polyketide compounds of mycobacterial origin as acyl-acceptor substrates. Overall, the results reported herein are in line with a model in which PapA5 catalyses the acylation of diol-containing polyketides to form PGLs. These studies advance our understanding of the biosynthesis of an important group of mycobacterial glycolipids and suggest that PapA5 might be an attractive target for exploring the development of antivirulence drugs.

Received 19 January 2012
Revised 15 February 2012
Accepted 18 February 2012

INTRODUCTION

The mycobacterial cell envelope contains a distinctive array of complex free lipids and glycolipids associated with the mycolic acid layer of the cell wall (Brennan & Nikaido, 1995; Crick *et al.*, 2008; Onwueme *et al.*, 2005a). These lipids and glycolipids are thought to be located in the membrane outer leaflet that partners with the mycolic acid-based membrane inner leaflet to form the asymmetric lipid bilayer that constitutes the characteristic mycobacterial outer membrane. Among the free lipids found in the outer membrane of *Mycobacterium leprae*, various strains of *Mycobacterium tuberculosis* and several opportunistic mycobacterial human pathogens are two structurally related groups of diesters, both composed of glycol-containing long-chain aliphatic polyketides and polyketide synthase-derived methyl-branched fatty acids (Onwueme *et al.*, 2005a). One of these groups of unusual lipid diesters is represented by phenolphthiocerol dimycocerosates, which are glycosylated compounds generally known as phenolic glycolipids (PGLs). The other group is represented by phthiocerol dimycocerosates (PDIMs), which lack the aromatic ring and glycosidic moieties characteristic of PGLs (Fig. 1).

An overwhelming body of evidence has accumulated that demonstrates that PGLs and PDIMs play important roles in host–pathogen interaction and/or virulence in various mycobacterial pathogens (Alibaud *et al.*, 2011; Astarie-Dequeker *et al.*, 2009; Brodin *et al.*, 2010; Camacho *et al.*, 1999; Collins *et al.*, 2005; Cox *et al.*, 1999; Dhungel *et al.*, 2008; Murry *et al.*, 2009; Ng *et al.*, 2000; Rambukkana *et al.*, 2002; Reed *et al.*, 2004; Robinson *et al.*, 2008; Ruley *et al.*, 2004; Sinsimer *et al.*, 2008; Tsenova *et al.*, 2005). Moreover, production of these compounds has been shown to correlate with decreased antimicrobial drug susceptibility (Alibaud *et al.*, 2011; Chavadi *et al.*, 2011b). PGL production has also been suggested as a trait that predisposes *M. tuberculosis* strains of the W-Beijing family to their characteristic epidemic spread and increased likelihood of developing drug resistance (Reed *et al.*,

†These authors contributed equally to this work.

‡Present address: North-West Hospital, 5401 Old Court Rd, Randallstown, MD 21133, USA.

Abbreviations: GPPOL, glycosyl-phenolphthiocerol; PDIM, phthiocerol dimycocerosate; PGL, phenolic glycolipid; SOE, splicing by overlap extension; WT, wild-type.

A supplementary figure, showing the construction of p2NIL-GOALc-Δ*papA5*c, is available with the online version of this paper.

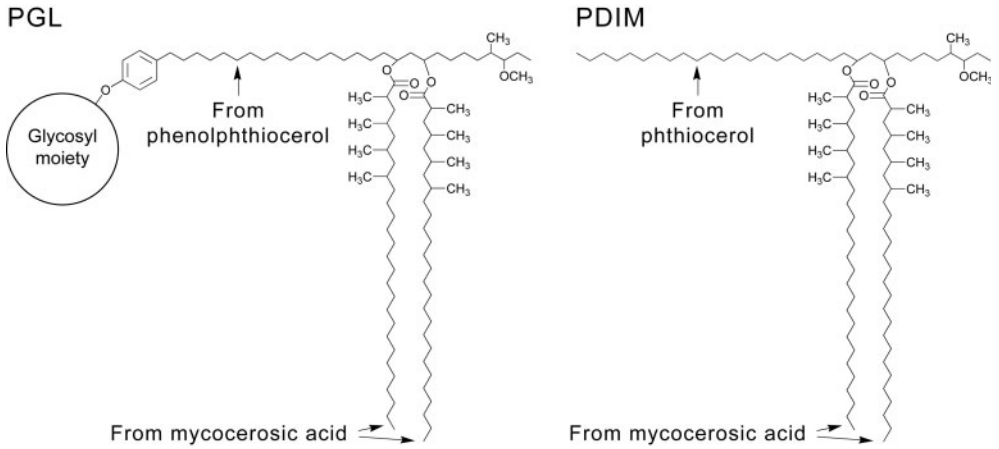

Fig. 1. Representative structures of mycobacterial PGLs and PDIMs.

2007). Thus, dissecting the molecular logic of PGL and PDIM biosynthesis not only will expand our general understanding of cell wall biosynthesis in mycobacteria of clinical significance, but also may reveal potential avenues for exploring the development of alternative therapeutics against selected mycobacterial infections (Ferreras *et al.*, 2008; Quadri, 2007). These views have directed our previous studies of the biosynthesis of PGLs and PDIMs (Buglino *et al.*, 2004; Chavadi *et al.*, 2011b; Ferreras *et al.*, 2008; He *et al.*, 2009; Onwueme *et al.*, 2004, 2005a, b), which include the development of the first PGL biosynthesis inhibitor (Ferreras *et al.*, 2008). This inhibitor drastically reduces PGL production in several *Mycobacterium* species (Ferreras *et al.*, 2008) using a mechanistic principle analogous to that of the first reported inhibitor of mycobacterial siderophore (iron chelator) production (Ferreras *et al.*, 2005; Quadri, 2007).

Despite significant progress made towards understanding the partially overlapping biosynthetic routes of PGLs and PDIMs (Onwueme *et al.*, 2005a), many aspects of these pathways remain unclear. One such aspect is whether the conserved gene *papA5* is required for PGL production. An orthologue of *papA5* is clustered with genes that have confirmed or suspected involvement in PGL and/or PDIM production in each PDIM/PGL producer for which the genome has been analysed (Onwueme *et al.*, 2005a). We have previously established that *papA5* is required for PDIM production, demonstrated that PapA5 has acyltransferase activity and reported the crystal structure of PapA5 from *M. tuberculosis* (Buglino *et al.*, 2004; Onwueme *et al.*, 2004). The earlier mutational work involved the characterization of a *papA5* knockout engineered in the Erdman strain of *M. tuberculosis*, a strain that is PGL-deficient due to a natural mutation in a polyketide synthase gene required for PGL synthesis (Constant *et al.*, 2002; He *et al.*, 2009). The study of PapA5 was conducted using non-physiological aliphatic alcohols as surrogate substrates. Thus, it remains unknown whether *papA5* is required for PGL production, and demonstration of the ability of PapA5 to utilize mycobacterial alcohols as acyl acceptor substrates is lacking.

In this study, we report a mutational analysis that conclusively establishes that *papA5* is required for production of PGLs in the opportunistic human pathogen *Mycobacterium marinum*. We also present *in vitro* biochemical evidence to demonstrate that PapA5 has the capacity to utilize mycobacterial glycosyl-phenolphthiocerols as acyl acceptor substrates. Overall, the studies reported herein advance our understanding of the biosynthesis of an important group of mycobacterial cell wall glycolipids.

METHODS

Chemicals and reagents. Solvents and non-radiolabelled chemical reagents were acquired from Sigma-Aldrich. [1-^{14}C]Palmitoyl-CoA thioester (specific activity 55–57 mCi mmol^{-1}; 2.04–2.11 GBq mmol^{-1}) was purchased from Perkin Elmer, Amersham Biosciences or American Radiolabelled Chemicals (ARC). [1-^{14}C]-propionate (specific activity 54 mCi mmol^{-1}; 2.00 GBq mmol^{-1}) was acquired from ARC. Molecular biology reagents were obtained from Sigma, Invitrogen, New England Biolabs, Novagen, Qiagen or Stratagene.

Bacterial culturing and recombinant DNA manipulations. *M. marinum* (strain M; ATCC BAA-535) was cultured at 30 °C in Middlebrook 7H9 medium (Difco) supplemented with 10 % ADN (5 % BSA, 2 % glucose, 0.85 % NaCl) (Difco) and 0.05 % Tween-80 (supplemented 7H9) or Middlebrook 7H11 (Difco) supplemented with ADN (supplemented 7H11) (Chavadi *et al.*, 2011b). *Escherichia coli* DH5α (Invitrogen) was cultured in Luria–Bertani media under standard conditions (Sambrook *et al.*, 1989). When required, kanamycin (30 μg ml^{-1}), hygromycin (50 μg ml^{-1}), sucrose (2 %) and/or X-Gal (70 μg ml^{-1}) were added to the media. General recombinant DNA manipulations were carried out by standard methods and using *E. coli* DH5α as the primary cloning host (Sambrook *et al.*, 1989). PCR-generated DNA fragments used in plasmid constructions were sequenced to verify fidelity. Genomic DNA isolation from and plasmid electroporation into mycobacteria were carried out as reported elsewhere (Parish & Stoker, 1998). The plasmids and oligonucleotides used in this study are shown in Table 1.

Table 1. Plasmids and oligonucleotide primers used in this study

Restriction sites are underlined.

Plasmid	Characteristics	Source or reference
pCR2.1Topo	Cloning vector, kanamycin and ampicillin resistance	Invitrogen
pCP0	*E. coli*–mycobacteria shuttle vector for gene expression in mycobacteria, kanamycin resistance	Ferreras *et al.* (2008)
pCP0-*papA5*mm	pCP0 expressing *M. marinum papA5* (*papA5*mm)	This study
p2NIL	Mutagenesis vector, kanamycin resistance	Parish & Stoker (2000)
pGOAL19	Mutagenesis vector, hygromycin resistance, *sacB–lacZ Pac*I cassette	Parish & Stoker (2000)
p2NIL-GOALc-Δ*papA5*c	Suicide delivery vector carrying *papA5* deletion cassette (Δ*papA5*c)	This study
Oligonucleotide	**Sequence (5′–3′)**	**Characteristics**
papA5OF	AAGCTTATCCTGGCGGACGCGGTTCGGATTCTGTTCA	*Hin*dIII site
papA5IR	CGCAGGTCATTCCATGAACACGTTAAGACTCTCCGTTCT	SOE primer
papA5IF	AGTCTTAACGTGTTCATGGAATGACCTGCGCCTGCG	SOE primer
papA5OR	TTAATTAAGTGGGCTGAGATGTTCCAGTCCAGTCCAGCGGTCAA	*Pac*I site
papA5F	CTGCAGGAAGAACGGAGAGTCTTAACGTGT	*Pst*I site
papA5R	AAGCTTGCAGGCGCAGGTCATTCCATGAAC	*Hin*dIII site

Construction of *M. marinum* Δ*papA5*. The mutant was engineered using the p2NIL/pGOAL19-based flexible cassette method (Parish & Stoker, 2000) as reported previously (Chavadi *et al.*, 2011a, b; Ferreras *et al.*, 2008; Onwueme *et al.*, 2004). A suicide delivery vector (p2NIL-GOALc-Δ*papA5*c, see below) carrying a *papA5* (MMAR_1768) deletion cassette (Δ*papA5*c) was used to generate *M. marinum* Δ*papA5*. Electroporation of p2NIL-GOALc-Δ*papA5*c into *M. marinum* and selection of potential single- and double-crossover mutants were conducted as previously reported (Chavadi *et al.*, 2011b). The *papA5* deletion in potential double-crossover mutants was screened for and confirmed by PCR using two independent primer pairs (papA5OF and papA5OR, papA5F and papA5R).

Construction of p2NIL-GOALc-Δ*papA5*c. The construction of the plasmid is outlined in Supplementary Fig. S1 (available with the online version of this paper). The deletion cassette Δ*papA5*c was generated using splicing by overlap extension (SOE) PCR (Horton *et al.*, 1989). Δ*papA5*c contained a 5′ arm (485 bp=479 bp segment upstream of *papA5*+*papA5* first two codons) and a 3′ arm (554 bp=*papA5* last two codons+stop codon+545 bp segment downstream of *papA5*). Each arm was PCR-generated from genomic DNA. Primer pair papA5OF and papA5IR and primer pair papA5IF and papA5OR were used to generate the 5′ and 3′ arms, respectively. The arms were then used as a template for PCR with primers papA5OF and papA5OR to fuse the arms and generate Δ*papA5*c (1039 bp). The PCR-generated Δ*papA5*c was cloned into pCR2.1Topo (Invitrogen). Δ*papA5*c was subsequently excised from the pCR2.1Topo construct using *Hin*dIII and *Pac*I, and the excerpt was ligated to plasmid p2NIL (Parish & Stoker, 2000) linearized by *Hin*dIII/*Pac*I digestion. The resulting p2NIL-Δ*papA5*c plasmid and plasmid pGOAL19 (Parish & Stoker, 2000) were digested with *Pac*I, and the *Pac*I cassette (GOALc, 7939 bp) of pGOAL19 was ligated to the linearized p2NIL-Δ*papA5*c backbone to create p2NIL-GOALc-Δ*papA5*c.

Construction of pCP0-*papA5*mm. A DNA fragment (1275 bp) encompassing *papA5* of *M. marinum* (*papA5*mm) and its predicted ribosome-binding site (RBS) was PCR-generated from genomic DNA using primer pair papA5F (starts and ends 20 nt upstream and 1 nt downstream, respectively, of the start codon) and papA5R (starts and ends 11 nt upstream and 10 nt downstream, respectively, of the stop codon). The PCR product was cloned into pCR2.1Topo. The RBS-*papA5*mm insert was recovered from the pCR2.1Topo construct as a *Pst*I–*Hin*dIII fragment and the excerpt was subcloned into the expression vector pCP0 linearized by *Pst*I/*Hin*dIII digestion. The cloned *papA5*mm was placed under the control of the *hsp60* promoter of pCP0 for expression in mycobacteria.

Analysis of PGLs and PDIMs. Five-day-old mycobacterial cultures were diluted to OD_{595} 0.6 in supplemented 7H9 and loaded into 12-well plates (1 ml per well). [^{14}C]Propionate was added to each well at 0.2 μCi ml^{-1} (7.4 MBq ml^{-1}) and the plates were incubated at 30 °C with rotary agitation (170 r.p.m.) for 24 h. After incubation, the OD_{595} of the cultures was measured in a DTX Plate Reader (Beckman Coulter), and the cells were harvested for apolar lipid fraction extraction with a biphasic mixture of methanolic saline and petroleum ether, as reported previously (Chavadi *et al.*, 2011b; Ferreras *et al.*, 2008). The lipid extracts were subjected to radio-TLC for analysis of ^{14}C-labelled PGLs (using $CHCl_3$/CH_3OH, 95 : 5) and PDIMs (using petroleum ether/diethyl ether, 9 : 1) as described previously (Ferreras *et al.*, 2008). Developed TLC plates were exposed to phosphor screens, which were scanned using a Cyclone Plus Storage Phosphor System (PerkinElmer Life and Analytical Sciences).

Purification of GPPOLs. PGLs were purified from *M. leprae*-infected Armadillo tissues. Briefly, homogenized *M. leprae* infected liver (10 g) supernatants were lyophilized and extracted with $CHCl_3$/CH_3OH (2 : 1) at 50 °C for 18 h. The homogenate was centrifuged and the organic layer (lower phase) was collected. This organic layer served as the main source of PGLs. The organic layer was washed with water, concentrated and extracted with diethyl ether. The ether-soluble dried lipids were resuspended in $CHCl_3$, applied to a silica gel G60 column (2.5 × 60 cm), and successively eluted from the column with $CHCl_3$ containing increasing concentrations of CH_3OH (0–20 %). Most of the PGL eluted with $CHCl_3$ containing 2 % and 5 % CH_3OH. The pure PGL preparation was obtained after normal-phase HPLC of the silica gel-purified material. Fractions off HPLC were screened for PGLs by TLC on aluminium-backed silica gel G plates (Merck) developed with $CHCl_3$/CH_3OH/H_2O (90 : 10 : 1). The identity of the purified PGLs was confirmed using fast atom bombardment MS (results not shown) as reported elsewhere (Brennan *et al.*, 1994). The purified PGLs were deacylated by procedures based on those described elsewhere (Hunter & Brennan, 1981). PGLs were hydrolysed with 10 % NaOH in toluene/CH_3OH

(1 : 2) in a sealed tube under N_2 at 100 °C for 18 h. Lipids were extracted with $CHCl_3$ from the water-diluted, acidified (pH 4) mixture. After two washes with water, the $CHCl_3$ fraction was applied to a column of silicic acid/celite (2 : 1) (1 × 30 cm), which was irrigated first with $CHCl_3$ to remove fatty acids and then with $CHCl_3$ containing 5 % CH_3OH to elute GPPOLs. The identity of the purified GPPOLs was confirmed by MS analysis as indicated below.

GPPOL palmitoylation assay. Reactions for assessment of PapA5-dependent GPPOL palmitoylation contained 18 μM [^{14}C]palmitoyl-CoA, 450 μM purified GPPOLs, 10 μM enzyme, 100 mM NaCl and 75 mM MES buffer (pH 6.2), and were incubated at 37 °C for 24 h. Negative control reactions contained the inactive PapA5 variant $PapH_{124}A$ (Onwueme *et al.*, 2004) or an equivalent volume of enzyme buffer (100 mM NaCl, 75 mM MES, pH 6.2). After incubation, the reactions were quenched by addition of $CHCl_3$/toluene/CH_3OH (6 : 4 : 2) followed by vigorous mixing. The organic layers were recovered and analysed by TLC on aluminium-backed, 250 μm thick, silica gel plates (EM Science or Whatman). TLC plates were developed with $CHCl_3/CH_3OH/H_2O$ (90 : 10 : 1) and exposed to phosphor screens, and reaction products were quantified with a Storm 860 Imaging System (Molecular Dynamics). For dose–response experiments, reactions contained GPPOLs at the indicated concentrations, 18 μM [^{14}C]palmitoyl-CoA, 0.5 μM PapA5, 100 mM NaCl and 75 mM MES, pH 6.5. After incubation (37 °C, 3 h), the reactions were quenched, extracted and analysed by radio-TLC as noted above. Dose–response data were fitted to the equation $v = V_{max}/[1 + K_m/S + S/K_i]$ to calculate apparent kinetic parameters and an apparent K_i value. Data were plotted and analysed using KaleidoGraph software. Recombinant PapA5 and $PapH_{124}A$ were purified as reported previously (Buglino *et al.*, 2004; Onwueme *et al.*, 2004).

MS analysis of GPPOL palmitoylation products. GPPOL palmitoylation reactions for MS analysis of reaction products contained unlabelled palmitoyl-CoA (360 μM), GPPOL (360 μM) and enzyme (90 μM), or an equivalent volume of the enzyme buffer described above in negative control reactions. Reactions were incubated at 37 °C for 24 h and then quenched and extracted as above. The organic extracts were analysed by MALDI-TOF MS. The analyte was mixed with matrix solution (10 mg 2,5-dihydroxybenzoic acid ml^{-1} in $CHCl_3/CH_3OH$, 1 : 1) and the resulting mix was applied onto the MALDI sample plate. Spectra were acquired on a Voyager-DE PRO 6320 instrument (Applied Biosystems). The instrument was calibrated using bradykinin fragment 1-7 (monoistopic mass 757.4), human angiotensin II (monoisotopic mass 1046.5) and a synthetic peptide $P_{14}R$ (monoisotopic mass 1533.8). The distributions in the spectra of the reactions were calibrated based on the main GPPOL species found in the purified substrate {observed $[(M+Na^+)]^+$ m/z=1123.79, calculated $[(M+Na^+)]^+$ m/z=1123.75}. Data were processed with the Data Explorer software package (Applied Biosystems).

RESULTS AND DISCUSSION

Construction of a *papA5* deletion mutant of *M. marinum*

We have previously demonstrated that *papA5* is required for production of PDIMs (Onwueme *et al.*, 2004). In this study, we sought to determine whether *papA5* was required for production of PGLs. Towards this end, we utilized *M. marinum* as a prototype representative of mycobacteria that produce both PGLs and PDIMs. *M. marinum* is an opportunistic human pathogen closely related to *M. tuberculosis* (Stinear *et al.*, 2008) and offers superior experimental tractability compared with other PGL-producing mycobacteria.

We engineered strain *M. marinum* Δ*papA5*, an unmarked, in-frame *papA5* deletion mutant of *M. marinum*, and examined the capacity of this strain to produce PGLs and PDIMs as described below. The deletion was engineered using the *papA5* deletion cassette-delivery suicide vector p2NIL-GOALc-Δ*papA5*c (Fig. 2a) in a homologous recombination- and counterselection-based approach that replaced *papA5* by a 4-codon remnant engineered into the *papA5* deletion cassette of p2NIL-GOALc-Δ*papA5*c. The deletion in *M. marinum* Δ*papA5* encompassed 412 central codons of *papA5*, and it was verified by PCR using two independent primer pairs, each producing diagnostic amplicons of different sizes depending on whether the genomic DNA used as template was wild-type (WT) or carried the *papA5* deletion (Fig. 2b). The successful engineering of *M. marinum* Δ*papA5* set the stage for probing the involvement of *papA5* in PGL production.

papA5 is required for production of both PGLs and PDIMs

We investigated the effect of the *papA5* deletion in *M. marinum* Δ*papA5* on PGL and PDIM production using published radio-TLC methods (see Methods). In addition, a control strain for genetic complementation analysis was constructed (*M. marinum* Δ*papA5* + pCP0-*papA5*mm, a plasmid expressing *papA5*mm), and the ability of this strain and that of *M. marinum* WT controls to produce PGLs and PDIMs was examined. We carried out metabolic labelling of mycobacterial cultures of these strains by feeding [^{14}C]propionate to obtain labelled PGLs and PDIMs for radio-TLC analysis. Representative results of this radio-TLC analysis are shown in Fig. 3. The analysis of lipid samples from *M. marinum* WT and *M. marinum* WT + pCP0 (empty vector control) revealed the presence of both PGLs and PDIMs, as expected based on previous reports (Ferreras *et al.*, 2008). More importantly, the analysis of samples from *M. marinum* Δ*papA5* and *M. marinum* Δ*papA5* + pCP0 indicated that deletion of *papA5* led not only to PDIM deficiency, a result expected based on the phenotype of *M. tuberculosis* Δ*papA5* (Onwueme *et al.*, 2004), but also to PGL deficiency. Introduction of pCP0-*papA5*mm into *M. marinum* Δ*papA5* complemented the mutant. The episomal expression of *papA5*mm restored PGL and PDIM production in *M. marinum* Δ*papA5* + pCP0-*papA5*mm to levels similar to those seen in *M. marinum* WT (Fig. 3). Overall, the results of the mutational analysis conclusively demonstrate that *papA5* is required for production of both PGLs and PDIMs in *M. marinum*.

PapA5 can catalyse acylation of mycobacterial diol-containing aliphatic polyketides *in vitro*

Using commercially available surrogate substrates we have previously demonstrated the capacity of *M. tuberculosis*

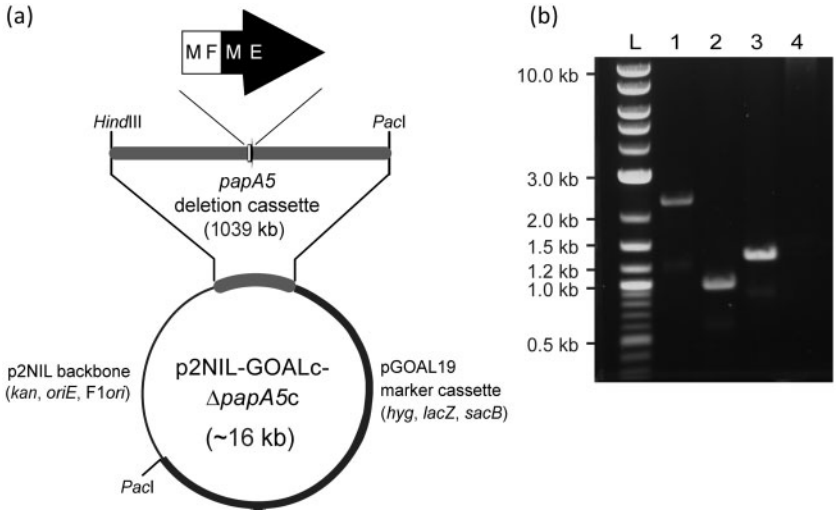

Fig. 2. Construction of *M. marinum* Δ*papA5*. (a) Scheme of *papA5* deletion cassette (Δ*papA5*c)-delivery suicide vector used for construction of *M. marinum* Δ*papA5*. The *papA5* deletion leaves behind a gene remnant consisting of the first two (black type) and last two (white type) amino acids of PapA5. The gene remnant in Δ*papA5*c is flanked by WT sequence for homologous recombination with the chromosome. (b) Agarose gel electrophoresis showing PCR-based confirmation of the *papA5* deletion in *M. marinum* Δ*papA5*. Lanes: 1, *M. marinum* WT (2270 bp amplicon expected with primers papA5OF and papA5OR); 2, *M. marinum* Δ*papA5* (1035 bp amplicon expected with papA5OF and papA5OR); 3, *M. marinum* WT (1275 bp amplicon expected with primers papA5F and papA5R); 4, *M. marinum* Δ*papA5* (no amplicon expected with papA5F and papA5R); L, DNA ladder marker.

PapA5 to catalyse hydroxyl-ester formation chemistry (Onwueme *et al.*, 2004). In these previous studies, surrogate alcohol and acyl-CoA thioester substrates replaced the suspected mycobacterial diol-containing aliphatic polyketide and multimethyl-branched fatty acyl thioester substrates, respectively, in the proposed esterification reactions catalysed by PapA5 (Buglino *et al.*, 2004; Onwueme *et al.*, 2004, 2005a). Herein, we set out to conduct a first examination of the ability of PapA5 to utilize mycobacterial diol-containing aliphatic polyketides as acyl acceptor substrates. To this end, we purified *M. leprae* PGL-derived GPPOLs to use as test substrates. *M. leprae* in infected Armadillo tissue produces PGLs in amounts that facilitate PGL isolation, and subsequent PGL hydrolytic deacylation and GPPOL purification (see Methods). The identity of the purified GPPOL preparation was verified by MS analysis. The mass spectrum of purified GPPOLs revealed the expected ion peak array, with a mass distribution pattern showing the 14 a.m.u. (-CH_2- unit) periodicity arising from the characteristic carbon chain-length heterogeneity in the phenolphthiocerol component of PGLs (Onwueme *et al.*, 2005a) (Fig. 4c). The main GPPOL species in the GPPOL preparation had an observed *m*/*z* of 1123.79. This *m*/*z* value is in agreement with the calculated *m*/*z* of 1123.75 for the sodium adduct $[(M+Na^+)]^+$ of the GPPOL species shown in Fig. 4(d). The availability of purified GPPOLs set the stage for a first examination of the competency of PapA5 to utilize a mycobacterial acyl acceptor substrate.

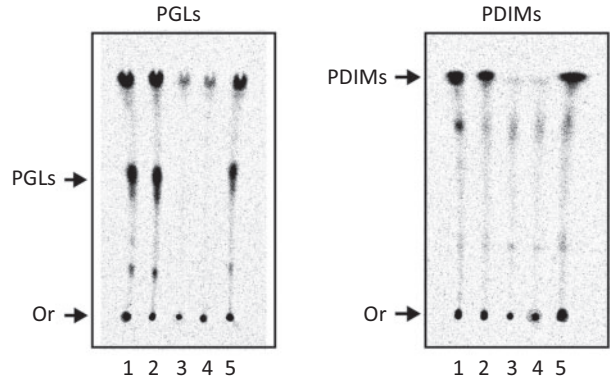

Fig. 3. PapA5 is required for production of both PGLs and PDIMs. Radio-TLC analysis of ^{14}C-labelled PGLs (with $CHCl_3/CH_3OH$, 95 : 5) and PDIMs (with petroleum ether/diethyl ether, 9 : 1). Lanes: 1, *M. marinum* WT; 2, *M. marinum* WT+pCP0; 3, *M. marinum* Δ*papA5*; 4, *M. marinum* Δ*papA5*+pCP0; 5, *M. marinum* Δ*papA5*+pCP0-*papA5*mm. Or, origin. Liquid chromatography-MS analysis (conducted as recently reported; Chavadi *et al.*, 2011b) demonstrated that the marginal signal in lanes 3 and 4 of the PDIM panel does not arise from PDIMs (not shown), but rather arises from other mycobacterial lipids that incorporate the label from [1-^{14}C]propionate.

We utilized a radio-TLC-based acyltransferase assay to investigate the ability of recombinant *M. tuberculosis* PapA5 to acylate purified GPPOLs *in vitro*. Representative results of this analysis are shown in Fig. 4(a, b). In these experiments, [^{14}C]palmitoyl-CoA was used as both a surrogate acyl donor substrate and a convenient radiotracer for visualization of [^{14}C]palmitoyl-derived ester products by radio-TLC analysis. Palmitoyl-CoA was selected as the acyl donor for these experiments because it is the most effective surrogate acyl donor among nearly 20 commercially available acyl-CoA thioesters tested as substrates of PapA5 (Onwueme *et al.*, 2004). TLC analysis

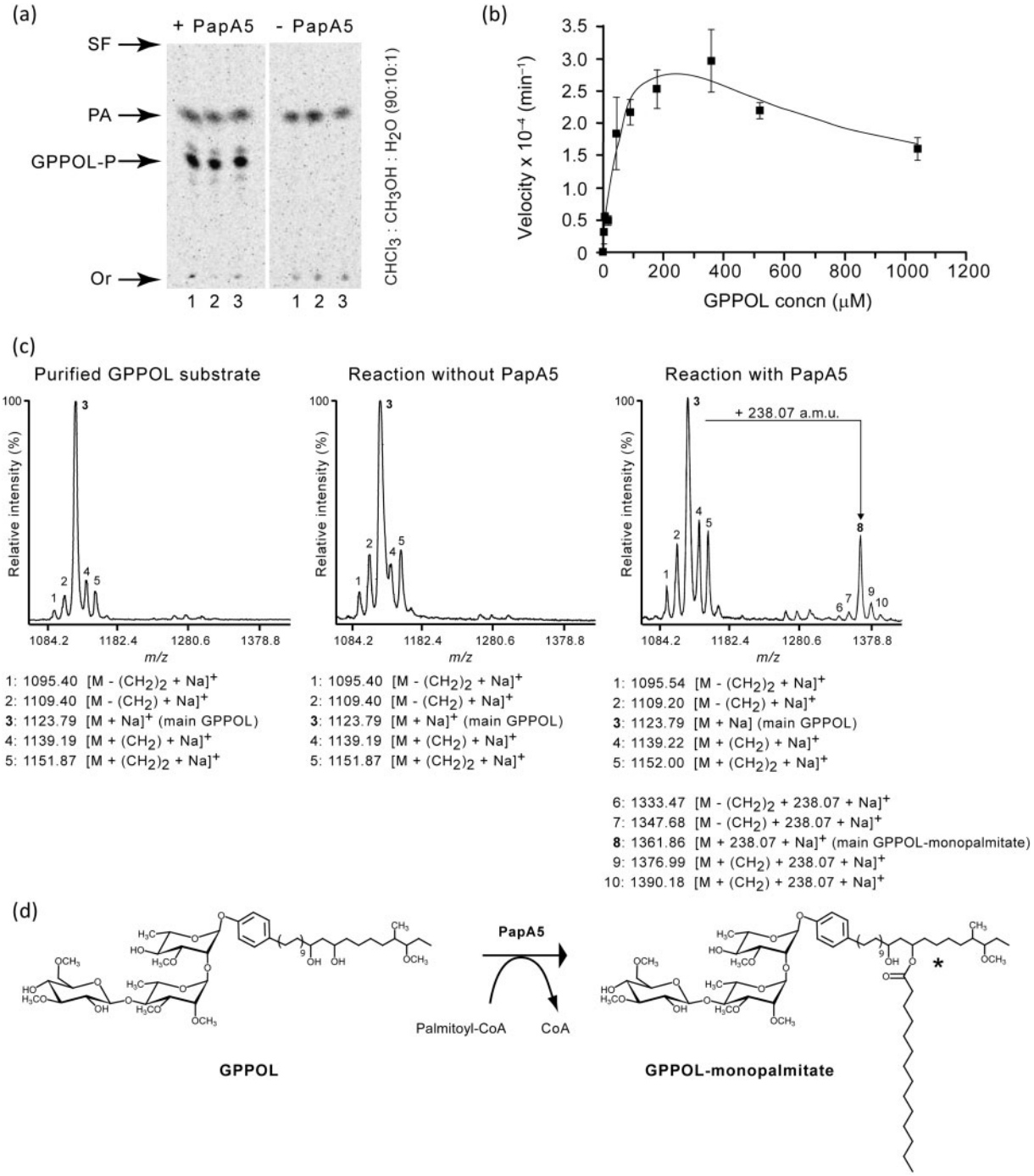

Fig. 4. PapA5-catalysed palmitoylation of GPPOLs *in vitro*. (a) Radio-TLC analysis showing PapA5-dependent formation of GPPOL-monopalmitate (GPPOL-P) esters. The main GPPOL-P product is marked. Each TLC panel shows triplicate reactions (lanes 1–3). The TLC solvent system is indicated. Or, origin; SF, solvent front; PA, palmitic acid. (b) Effect of GPPOL concentration on the rate of PapA5-catalysed GPPOL-monopalmitate formation. Means ± SEM of triplicate reactions are shown. (c) MS analysis demonstrating PapA5-dependent palmitoylation of GPPOLs. The spectra show ion peak arrays with *m/z* values arising from the natural structural heterogeneity in the phenolphthiocerol component of PGLs. (d) Scheme of the proposed GPPOL palmitoylation reaction catalysed by PapA5. Only the main GPPOL species is displayed. The asterisk indicates that only one of two possible regioisomers is shown.

of reactions with PapA5, purified GPPOLs and [^{14}C]palmitoyl-CoA revealed the formation of two main labelled products (Fig. 4a). The product with the higher R_f is palmitate, which is known to be formed by non-specific hydrolysis of [^{14}C]palmitoyl-CoA under our reaction conditions (Onwueme *et al.*, 2004). The product with the lower R_f was formed only in reactions containing both PapA5 and substrates. Formation of the lower R_f product was not detected in reactions lacking PapA5 (Fig. 4a), in reactions without GPPOL (Onwueme *et al.*, 2004), or in reactions with the PapA5 variant PapH_{124}A in place of PapA5 (not shown). PapH_{124}A has the catalytic residue His-124 replaced by Ala and lacks acyltransferase activity (Buglino *et al.*, 2004; Onwueme *et al.*, 2004). We reasoned that the lower R_f product was emerging from PapA5-catalysed palmitoylation of GPPOL, and indeed MS analysis supported the identity of the product as GPPOL-monopalmitate (see below). Notably, the TLC analysis revealed the presence of two less abundant products flanking the lower R_f product (hereafter referred to as GPPOL-monopalmitate). These secondary products are likely to arise from formation of GPPOL-monopalmitates with carbon chain-length heterogeneity in the GPPOL component (Fig. 4c). This view is in agreement with the results of the MS analysis described below. PapA5-dependent formation of GPPOL-monopalmitate was dependent on the concentration of GPPOLs in the reaction mixture, and an apparent substrate inhibition effect was observed at high levels of GPPOLs in the reaction (Fig. 4b). Apparent V_{max}, K_m and K_i values determined from these data were 5×10^{-4} min^{-1}, 103 μM and 496 μM, respectively.

We probed the PapA5-dependent formation of GPPOL-palmitate esters by MS. Comparative analysis of mass spectra obtained from reactions containing PapA5 and the mass spectra of negative control reactions (no enzyme) validated the PapA5-dependent formation of GPPOL-monopalmitate (Fig. 4c). As expected, the mass spectra of both PapA5-containing and negative control reactions displayed an ion peak array with the mass distribution characteristic of the purified GPPOLs. Most importantly, an ion peak array centred at m/z=1361.86 was detected only in reactions containing PapA5. This m/z value corresponds to the sodium adduct $[(M+Na^+)]^+$ of the main GPPOL species present in the purified GPPOL preparation plus the addition of 238.07 a.m.u. This mass gain is concordant with the expected acylation of the main GPPOL species with a palmitoyl chain to form GPPOL-monopalmitate (Fig. 4d). The additional ion peaks in the array had m/z values that matched those predicted for the sodium adducts of monopalmitate esters derived from secondary GPPOL species present in the GPPOL preparation. Formation of polyacylated GPPOLs was not detected by MS. PapA5 is expected to acylate both hydroxyl groups in the diol of the phenolphthiocerol chains during *in vivo* PGL biosynthesis. The *in vitro* observed monopalmitoylation is not surprising considering that the use of a non-physiological acyl donor substrate and the lack of potentially relevant factors (protein partners, possibility of membrane association) in the acylation assay might affect the processivity and kinetic parameters of PapA5.

The ability of PapA5 to acylate GPPOLs of different carbon chain length *in vitro* is in line with the proposed role of this enzyme in the biosynthesis of PGLs with carbon chain-length variability in the phenolphthiocerol moiety. Due to the inability of the PapA5 active site cavity to accommodate the bulky oligosaccharide unit of GPPOL (Buglino *et al.*, 2004), and since PapA5 acylates alkanol and alkanediol surrogate substrates with a hydrophobic character but not sugars (Onwueme *et al.*, 2004), we propose that the observed palmitoylation is likely to take place at one of the hydroxyl groups of the diol of phenolphthiocerol (Fig. 4d). Future studies will be required to validate this prediction, which is consistent with the hypothesized physiological acylation target of PapA5.

In conclusion, the results of both the *in vivo* mutational analysis and the *in vitro* biochemical studies presented herein are in line with a model in which PapA5 catalyses the acylation of diol-containing aliphatic polyketides with multimethyl branched fatty acids during biosynthesis of PGLs. The enzymic assay developed herein will provide a basis for more advanced studies of PapA5 activity, whereas the availability of *M. marinum* Δ*papA5* will facilitate future studies of biosynthetic intermediate accumulation. Overall, our studies advance the understanding of the biosynthesis of an important group of mycobacterial cell wall glycolipids and suggest that PapA5 might be an attractive target for the development of drugs that inhibit the biosynthesis of both PGLs and PDIMs. Such antivirulence drugs might be combined with conventional antimicrobial drugs in the treatment of selected mycobacterial infections.

ACKNOWLEDGEMENTS

This work was supported by NIH/NIAID grant R01AI069209 to L. E. N. Q. L. E. N. Q. acknowledges the endowment support from Carol and Larry Zicklin. We are grateful to Albert Morrishow (Weill Medical College) for assistance with MS analysis, Professor Christopher Lima (Memorial Sloan-Kettering Cancer Center) for providing PapA5, and Catherine Chan (Quadri laboratory) for help with plasmid constructions. K. C. O. was supported by NIH/MSTP grant GM07739, Minority Predoctoral Fellowship AI054326, and a United Negro College Fund-Merck Fellowship. D. C. was supported in part by NIH/NIAID contract N01 AI-25469.

REFERENCES

Alibaud, L., Rombouts, Y., Trivelli, X., Burguière, A., Cirillo, S. L., Cirillo, J. D., Dubremetz, J. F., Guérardel, Y., Lutfalla, G. & Kremer, L. (2011). A *Mycobacterium marinum* TesA mutant defective for major cell wall-associated lipids is highly attenuated in *Dictyostelium discoideum* and zebrafish embryos. *Mol Microbiol* **80**, 919–934.

Astarie-Dequeker, C., Le Guyader, L., Malaga, W., Seaphanh, F. K., Chalut, C., Lopez, A. & Guilhot, C. (2009). Phthiocerol dimycocerosates

of *M. tuberculosis* participate in macrophage invasion by inducing changes in the organization of plasma membrane lipids. *PLoS Pathog* **5**, e1000289.

Brennan, P. J. & Nikaido, H. (1995). The envelope of mycobacteria. *Annu Rev Biochem* **64**, 29–63.

Brennan, P. J., Chatterjee, D., Fujiwara, T. & Cho, S. N. (1994). Leprosy-specific neoglycoconjugates: synthesis and application to serodiagnosis of leprosy. *Methods Enzymol* **242**, 27–37.

Brodin, P., Poquet, Y., Levillain, F., Peguillet, I., Larrouy-Maumus, G., Gilleron, M., Ewann, F., Christophe, T., Fenistein, D. & other authors (2010). High content phenotypic cell-based visual screen identifies *Mycobacterium tuberculosis* acyltrehalose-containing glycolipids involved in phagosome remodeling. *PLoS Pathog* **6**, e1001100.

Buglino, J., Onwueme, K. C., Ferreras, J. A., Quadri, L. E. & Lima, C. D. (2004). Crystal structure of PapA5, a phthiocerol dimycocerosyl transferase from *Mycobacterium tuberculosis*. *J Biol Chem* **279**, 30634–30642.

Camacho, L. R., Ensergueix, D., Perez, E., Gicquel, B. & Guilhot, C. (1999). Identification of a virulence gene cluster of *Mycobacterium tuberculosis* by signature-tagged transposon mutagenesis. *Mol Microbiol* **34**, 257–267.

Chavadi, S. S., Stirrett, K. L., Edupuganti, U. R., Vergnolle, O., Sadhanandan, G., Marchiano, E., Martin, C., Qiu, W. G., Soll, C. E. & Quadri, L. E. (2011a). Mutational and phylogenetic analyses of the mycobacterial *mbt* gene cluster. *J Bacteriol* **193**, 5905–5913.

Chavadi, S. S., Edupuganti, U. R., Vergnolle, O., Fatima, I., Singh, S. M., Soll, C. E. & Quadri, L. E. (2011b). Inactivation of *tesA* reduces cell wall lipid production and increases drug susceptibility in mycobacteria. *J Biol Chem* **286**, 24616–24625.

Collins, D. M., Skou, B., White, S., Bassett, S., Collins, L., For, R., Hurr, K., Hotter, G. & de Lisle, G. W. (2005). Generation of attenuated *Mycobacterium bovis* strains by signature-tagged mutagenesis for discovery of novel vaccine candidates. *Infect Immun* **73**, 2379–2386.

Constant, P., Perez, E., Malaga, W., Lanéelle, M. A., Saurel, O., Daffé, M. & Guilhot, C. (2002). Role of the *pks15/1* gene in the biosynthesis of phenolglycolipids in the *Mycobacterium tuberculosis* complex. Evidence that all strains synthesize glycosylated *p*-hydroxybenzoic methyl esters and that strains devoid of phenolglycolipids harbor a frameshift mutation in the *pks15/1* gene. *J Biol Chem* **277**, 38148–38158.

Cox, J. S., Chen, B., McNeil, M. & Jacobs, W. R., Jr (1999). Complex lipid determines tissue-specific replication of *Mycobacterium tuberculosis* in mice. *Nature* **402**, 79–83.

Crick, D. C., Quadri, L. E. & Brennan, P. J. (2008). Biochemistry of the cell envelope of *Mycobacterium tuberculosis*. In *Handbook of Tuberculosis: Molecular Biology and Biochemistry*, pp. 1–19. Edited by S. H. E. Kaufmann & R. Rubin. Weinheim: Wiley-VCH.

Dhungel, S., Ranjit, C., Sapkota, B. R. & Macdonald, M. (2008). Role of PGL-I of *M. leprae* in TNF-alpha production by *in vitro* whole blood assay. *Nepal Med Coll J* **10**, 1–3.

Ferreras, J. A., Ryu, J. S., Di Lello, F., Tan, D. S. & Quadri, L. E. (2005). Small-molecule inhibition of siderophore biosynthesis in *Mycobacterium tuberculosis* and *Yersinia pestis*. *Nat Chem Biol* **1**, 29–32.

Ferreras, J. A., Stirrett, K. L., Lu, X., Ryu, J. S., Soll, C. E., Tan, D. S. & Quadri, L. E. (2008). Mycobacterial phenolic glycolipid virulence factor biosynthesis: mechanism and small-molecule inhibition of polyketide chain initiation. *Chem Biol* **15**, 51–61.

He, W., Soll, C. E., Chavadi, S. S., Zhang, G., Warren, J. D. & Quadri, L. E. (2009). Cooperation between a coenzyme A-independent stand-alone initiation module and an iterative type I polyketide synthase during synthesis of mycobacterial phenolic glycolipids. *J Am Chem Soc* **131**, 16744–16750.

Horton, R. M., Hunt, H. D., Ho, S. N., Pullen, J. K. & Pease, L. R. (1989). Engineering hybrid genes without the use of restriction enzymes: gene splicing by overlap extension. *Gene* **77**, 61–68.

Hunter, S. W. & Brennan, P. J. (1981). A novel phenolic glycolipid from *Mycobacterium leprae* possibly involved in immunogenicity and pathogenicity. *J Bacteriol* **147**, 728–735.

Murry, J. P., Pandey, A. K., Sassetti, C. M. & Rubin, E. J. (2009). Phthiocerol dimycocerosate transport is required for resisting interferon-γ-independent immunity. *J Infect Dis* **200**, 774–782.

Ng, V., Zanazzi, G., Timpl, R., Talts, J. F., Salzer, J. L., Brennan, P. J. & Rambukkana, A. (2000). Role of the cell wall phenolic glycolipid-1 in the peripheral nerve predilection of *Mycobacterium leprae*. *Cell* **103**, 511–524.

Onwueme, K. C., Ferreras, J. A., Buglino, J., Lima, C. D. & Quadri, L. E. (2004). Mycobacterial polyketide-associated proteins are acyltransferases: proof of principle with *Mycobacterium tuberculosis* PapA5. *Proc Natl Acad Sci U S A* **101**, 4608–4613.

Onwueme, K. C., Vos, C. J., Zurita, J., Ferreras, J. A. & Quadri, L. E. (2005a). The dimycocerosate ester polyketide virulence factors of mycobacteria. *Prog Lipid Res* **44**, 259–302.

Onwueme, K. C., Vos, C. J., Zurita, J., Soll, C. E. & Quadri, L. E. (2005b). Identification of phthiodiolone ketoreductase, an enzyme required for production of mycobacterial diacyl phthiocerol virulence factors. *J Bacteriol* **187**, 4760–4766.

Parish, T. & Stoker, N. G. (1998). *Mycobacteria Protocols*. Totowa, NJ: Humana Press.

Parish, T. & Stoker, N. G. (2000). Use of a flexible cassette method to generate a double unmarked *Mycobacterium tuberculosis tlyA plcABC* mutant by gene replacement. *Microbiology* **146**, 1969–1975.

Quadri, L. E. N. (2007). Strategic paradigm shifts in the antimicrobial drug discovery process of the 21st century. *Infect Disord Drug Targets* **7**, 230–237.

Rambukkana, A., Zanazzi, G., Tapinos, N. & Salzer, J. L. (2002). Contact-dependent demyelination by *Mycobacterium leprae* in the absence of immune cells. *Science* **296**, 927–931.

Reed, M. B., Domenech, P., Manca, C., Su, H., Barczak, A. K., Kreiswirth, B. N., Kaplan, G. & Barry, C. E., III (2004). A glycolipid of hypervirulent tuberculosis strains that inhibits the innate immune response. *Nature* **431**, 84–87.

Reed, M. B., Gagneux, S., Deriemer, K., Small, P. M. & Barry, C. E., III (2007). The W-Beijing lineage of *Mycobacterium tuberculosis* overproduces triglycerides and has the DosR dormancy regulon constitutively upregulated. *J Bacteriol* **189**, 2583–2589.

Robinson, N., Kolter, T., Wolke, M., Rybniker, J., Hartmann, P. & Plum, G. (2008). Mycobacterial phenolic glycolipid inhibits phagosome maturation and subverts the pro-inflammatory cytokine response. *Traffic* **9**, 1936–1947.

Ruley, K. M., Ansede, J. H., Pritchett, C. L., Talaat, A. M., Reimschuessel, R. & Trucksis, M. (2004). Identification of *Mycobacterium marinum* virulence genes using signature-tagged mutagenesis and the goldfish model of mycobacterial pathogenesis. *FEMS Microbiol Lett* **232**, 75–81.

Sambrook, J., Fritsch, E. F. & Maniatis, T. (1989). *Molecular Cloning: a Laboratory Manual*, 2nd edn. Cold Spring Harbor, NY: Cold Spring Harbor Laboratory.

Sinsimer, D., Huet, G., Manca, C., Tsenova, L., Koo, M. S., Kurepina, N., Kana, B., Mathema, B., Marras, S. A. & other authors (2008). The phenolic glycolipid of *Mycobacterium tuberculosis* differentially

modulates the early host cytokine response but does not in itself confer hypervirulence. *Infect Immun* **76**, 3027–3036.

Stinear, T. P., Seemann, T., Harrison, P. F., Jenkin, G. A., Davies, J. K., Johnson, P. D., Abdellah, Z., Arrowsmith, C., Chillingworth, T. & other authors (2008). Insights from the complete genome sequence of *Mycobacterium marinum* on the evolution of *Mycobacterium tuberculosis*. *Genome Res* **18**, 729–741.

Tsenova, L., Ellison, E., Harbacheuski, R., Moreira, A. L., Kurepina, N., Reed, M. B., Mathema, B., Barry, C. E., III & Kaplan, G. (2005). Virulence of selected *Mycobacterium tuberculosis* clinical isolates in the rabbit model of meningitis is dependent on phenolic glycolipid produced by the bacilli. *J Infect Dis* **192**, 98–106.

Edited by: R. Manganelli